The University of Sydney
Department of Civil Engineering
Sydney NSW 2006
AUSTRALIA

http://www.civil.usyd.edu.au/

Centre for Advanced Structural Engineering

Design of Angle Columns with Locally Unstable Legs

Research Report No R830

By

Kim JR Rasmussen MScEng PhD

June 2003

The University of Sydney

Department of Civil Engineering
Centre for Advanced Structural Engineering
http://www.civil.usyd.edu.au

Design of Angle Columns with Locally Unstable Legs

Research Report No. R830

Kim JR Rasmussen MScEng PhD

June 2003

Abstract:

The report is concerned with angle section columns whose legs are slender and thus subject to local buckling in their ultimate limit state. For such slender angle sections, the local buckling mode is identical to the torsional mode and traditional design procedures become excessively conservative because they account for the torsional (local) buckling mode twice. The report describes design methods for slender equal angles which ignore torsion in determining the overall buckling stress and uses recently presented effective width equations to accurately determining the bending capacity of angle sections, as required in the beam-column design approach. The shift in the effective centroid resulting from local buckling is determined from the actual stress distribution, as obtained using Stowell's classical solution, rather than the effective cross-section. Having validated the design procedure against tests on slender equal angles, the same procedure is applied to slender unequal angles. The columns are assumed to be simply supported and thus allowed to rotate about their principal axes.

Keywords:

Angles, columns, beam-columns, local buckling, flexural buckling, flexural-torsional buckling, design, shift of the effective centroid.

Department of Civil Engineering, Research Report R830
Design of Angle Columns with Locally Unstable Legs

k.rasmussen@civil.usyd.edu.au

Published by:
Department of Civil Engineering
The University of Sydney
Sydney, NSW, 2006
AUSTRALIA

June 2003

http://www.civil.usyd.edu.au

Table of contents

1 Introduction

This report concerns angles whose legs are *slender* and hence prone to local buckling in their ultimate limit state. Traditionally, angles were hot-rolled and generally fully effective, *ie* capable of supporting the full yield stress in compression. However, angles are increasingly being manufactured by cold-forming, and cross-sections are becoming increasing slender. It is now common to find standard slender sections in product catalogues of cold-formed angles.

The warping constant (I_w) of angles is negligible and is derived only from secondary warping and, in the case of cold-formed angles, the effect of rounded corners. Consequently, angles are weak in torsion, and the common overall buckling mode is a flexural-torsional mode at short and intermediate lengths, which may change to a minor axis flexural mode at intermediate and long lengths for an equal angle. At short lengths, the flexural-torsional buckling load approaches the torsional buckling load, which, for an equal angle, is identical to the local buckling mode, as shown in the following section. Slender equal angles, therefore, pertain to the unique class of sections for which the local buckling mode is the same as the critical overall bucking mode at short lengths. Conventional design procedures become excessively conservative for this class of sections because they account for the torsional (local) mode twice: through the member strength provisions and through the effective width provisions.

Further complications arise as a result of local buckling of a slender section: The stress redistributes in the section and the resultant of the stress becomes eccentric to the centroid (C), as shown in Figs 1a-c. In a concentrically loaded pin-ended column, the eccentricity (e_0), referred to as the shift in the effective centroid (C_e), leads to overall bending (Rhodes and Harvey 1977) because the external load becomes eccentric to the internal stress resultant under uniform compression, implying that local buckling must be accompanied by overall bending. The column also becomes sensitive to small eccentricities of loading. A load applied with an eccentricity (e_P) towards the free edge of the flanges (Fig. 1d) can significantly reduce the strength of the column because it triggers local buckling at a reduced load. Conversely, applying the load towards the corner enhances the strength for moderate eccentricities.

To account for the effect of the shift in the effective centroid, current provisions of the North American Specification (NAS 2000) and the Australian Cold-formed Steel Structures Standard (AS/NZS4600 1996) specify that slender angle columns are to be considered concentrically loaded when the force passes through the *effective* centroid, rather than the gross section centroid. Furthermore, it is required to account for an additional moment of $P \times L/1000$[1]. As a result, slender angle columns are inevitably required to be designed as beam-columns.

[1] The additional moment is also required to be applied to non-slender angels in the 1997 edition of the AISI Specification and the 1996 edition of AS/NZS4600. However, research Popovic et al. (1999) has shown that the additional moment is not required for non-slender angles and amendments to these specifications have recently been balloted which now only require the eccentricity to be applied to slender angles.

In designing an angle strut as a beam-column, it is required to compute the bending capacity, which for a slender angle involves determining the effective width of a flange element (or unstiffened element) under stress gradient. Current provisions (AS/NZS4600 1996; NAS 2000) conservatively treat unstiffened elements under stress gradient as if subjected to uniform compression. This procedure leads to low bending capacities and hence conservative beam-column capacities. However, recent research (Bambach and Rasmussen 2002b; a) has produced accurate effective width equations for unstiffened elements under stress gradient, as described in the following sections. The objective of this paper is to demonstrate how the improved effective width equations can be combined with a simple equation for the eccentricity (e_0) induced by the shift of the effective centroid to produce an accurate design procedure for slender angles.

The report first develops a design procedure for slender equal angle columns. Subsequently, the same procedure is applied to unequal angles, leading to an interaction equation involving bending about both principal axes.

2 Elastic buckling loads for equal angles

2.1. Compression

According to classical theory (Timoshenko 1945; Chajes and Winter 1965), the flexural-torsional buckling stress of a simply supported singly symmetric column is given by,

$$F_{ext} = \frac{(\sigma_{ex} + \sigma_{et}) \pm \sqrt{(\sigma_{ex} + \sigma_{et})^2 - 4\sigma_{ex}\sigma_{et}\left(1 - \frac{x_0^2}{r_0^2 + x_0^2}\right)}}{2\left(1 - \frac{x_0^2}{r_0^2 + x_0^2}\right)} \tag{1}$$

where σ_{ex} and σ_{et} are the major axis flexural and torsional buckling stresses respectively, x_0 is the distance from the centroid (C) to the shear centre (S), as shown in Fig. 2, and r_0 is the polar radius of gyration, as follows

$$\sigma_{ex} = \frac{\pi^2 E I_x}{A(K_x L)^2} \tag{2}$$

$$\sigma_{et} = \left(\frac{\pi^2 E I_w}{(K_t L)^2} + GJ\right) / \left[A(r_0^2 + x_0^2)\right] \tag{3}$$

$$r_0^2 = \frac{I_P}{A} = \frac{I_x + I_y}{A}. \tag{4}$$

In eqns (2-4), E is the elastic modulus, G is the shear modulus, A is the area, I_x and I_y are the second moments of area about the x and y axes respectively, J is the torsion constant, I_w is the warping constant, and K_t and K_x are the effective lengths factors for torsion and bending about the x-axis respectively.

When, as for angles, $I_w \approx 0$, the torsional buckling stress reduces to

$$\sigma_{et} = GJ / \left[A\left(r_0^2 + x_0^2\right)\right] \tag{5}$$

which, on using that for an equal angle with sharp corners (see Fig. 2 for notations),

$$r_0^2 = \frac{5}{24}B^2 \qquad x_0^2 = \frac{1}{8}B^2 \qquad J = \frac{2}{3}Bt^3 \qquad G = \frac{E}{2(1+\nu)} \tag{6}$$

simplifies further to,

$$\sigma_{et} = \frac{E}{2(1+\nu)}\left(\frac{t}{B}\right)^2. \tag{7}$$

The local buckling stress for an equal angle section is exactly the same as that for a single plate which is simply supported along three edges with one longitudinal edge free. The characteristic equation for such a plate is (Bulson 1969),

$$qr^4 \sinh(p)\cos(q) - ps^4 \cosh(p)\sin(q) = 0 \tag{8}$$

where

$$p = \left[\frac{\pi^2}{\varphi}\left(\sqrt{k} + \frac{1}{\varphi}\right)\right]^{\frac{1}{2}} \qquad q = \left[\frac{\pi^2}{\varphi}\left(\sqrt{k} - \frac{1}{\varphi}\right)\right]^{\frac{1}{2}} \tag{9}$$

$$r^4 = \left[p^2 - \frac{\nu\pi^2}{\varphi^2}\right]^2 \qquad s^4 = \left[p^2 + \frac{\nu\pi^2}{\varphi^2}\right]^2. \tag{10}$$

In eqns (9,10), k is the plate buckling coefficient and ϕ is the plate aspect ratio,

$$\varphi = \frac{L}{B}. \tag{11}$$

Equation (8) does not have a general closed form solution but for $L \to \infty$ leads to,

$$k = \frac{6(1-\nu)}{\pi^2} \tag{12}$$

which, upon substitution into the expression for the local buckling stress,

$$F_{cr} = \frac{k\pi^2 E}{12(1-\nu^2)}\left(\frac{t}{B}\right)^2 \tag{13}$$

reproduces eqn. (7) exactly. Thus, the asymptotic value of the local buckling stress equals the torsional buckling stress. For finite aspect ratios, the plate buckling coefficient can be approximated by (Bulson 1969),

$$k = \frac{6(1-\nu)}{\pi^2} + \frac{1}{\varphi^2}. \tag{14}$$

This expression converges rapidly to the asymptotic value $(6(1\text{-}\nu)/\pi^2)$ and hence, it can be assumed that the local buckling stress and the torsional buckling stress are equal for practical lengths of equal angle columns.

2.2. Bending

For a singly symmetric column bent in the plane of symmetry, the compression stress to cause flexural-torsional buckling is given by,

$$F_{eb} = \frac{C_s A \sigma_{ex}}{C_{TF} S_f}\left(j + C_s\sqrt{j^2 + (r_0^2 + x_0^2)\sigma_{et}/\sigma_{ex}}\right) \tag{15}$$

where A is the area, S_f is the elastic modulus of the full cross-section, σ_{ex} is the flexural buckling stress for bending about the x-axis, C_{TF} is a moment distribution factor, which is unity for a beam in uniform bending, and j is the monosymmetry parameter defined as,

$$j = \frac{1}{2I_y}\left[\int_A x^3 dA + \int_A xy^2 dA\right] - x_0. \tag{16}$$

The factor C_s in eqn. (15) equals –1 when bending causes tension on the shear centre side and +1 when it causes compression. For equal angles with sharp corners, the torsional buckling stress (σ_{et}) is given by eqn. (5), and

$$A = 2Bt \qquad S_f = \frac{\sqrt{2}}{6}tB^2 \qquad j = B/\sqrt{2} \qquad \sigma_{ex} = \frac{\pi^2 E}{(K_x L/r_x)^2}. \tag{17}$$

On substituting eqns (5,6,17) into eqn. (15), the following buckling stresses are obtained,

$$\frac{F_{eb,t}}{\sigma_{et}} = \frac{4}{\alpha\left(\frac{L}{B}\right)^2}\left[\sqrt{1+\alpha\left(\frac{L}{B}\right)^2} - 1\right] \tag{18}$$

$$\frac{F_{eb,c}}{\sigma_{et}} = \frac{4}{\alpha\left(\frac{L}{B}\right)^2}\left[\sqrt{1+\alpha\left(\frac{L}{B}\right)^2} + 1\right] \tag{19}$$

where $F_{eb,t}$ and $F_{eb,c}$ are the compressive stresses at the tips of the flanges and corner respectively, as shown in Figs 3a and 3b respectively, and

$$\alpha = \frac{2}{\pi^2(1+\nu)}\left(\frac{t}{B}\right)^2. \tag{20}$$

Figures 3a and 3b shows graphs of $F_{eb,t}$ and $F_{eb,c}$ versus L/B for $\alpha=10^{-5}$, 10^{-4} and 10^{-3}, covering the range from slender to stocky angles. In the limit $L/B \to 0$, the buckling stress $F_{eb,t}$ approaches $2\sigma_{et}$, *ie* for short angles, the flexural-torsional buckling stress becomes the torsional buckling stress for bending which is twice the torsional buckling stress for uniform compression.

As shown in Figs 3a and 3b, the buckling stress ($F_{eb,c}$) for an equal angle beam subjected to compression at the corner is an order of magnitude higher than the buckling stress $F_{eb,t}$ corresponding to compression at the tips. In practical terms, an equal angle beam subjected to compression at the corner will usually fail by yielding before buckling in a flexural-torsional mode.

3 Design provisions for equal angles

3.1. Current NAS Specification and AS/NZS4600

Compression

According to the American and Australian specifications for cold-formed steel structures (AS/NZS4600 1996; NAS 2000), the inelastic column buckling strength of an equal angle is determined as,

$$F_n = \begin{cases} \left[0.658^{\lambda_c^2}\right] F_y & \text{for } \lambda_c \le 1.5 \\ \left[\frac{0.877}{\lambda_c^2}\right] F_y & \text{for } \lambda_c > 1.5 \end{cases} \tag{21}$$

$$\lambda_c = \sqrt{\frac{F_y}{F_e}} \tag{22}$$

where F_e=min{F_{ext}, σ_{ey}} is the lower of flexural-torsional buckling stress given by eqn. (1) and the flexural buckling stress,

$$\sigma_{ey} = \frac{\pi^2 E I_y}{A(K_y L)^2}. \tag{23}$$

The effective widths are determined as,

$$b_e = \rho w \tag{24}$$

$$\rho = \begin{cases} 1 & \text{for } \lambda_p \le 0.673 \\ (1 - 0.22/\lambda_p)/\lambda_p & \text{for } \lambda_p > 0.673 \end{cases} \tag{25}$$

where w is the flat width, as shown in Fig. 4 for an equal angle with a rounded corner, and λ_p is the plate slenderness calculated at the column buckling stress (f=F_n),

$$\lambda_p = \sqrt{\frac{f}{F_{cr}}}. \tag{26}$$

For angles, the elastic plate buckling stress (F_{cr}) is determined using eqn. (13) with k=0.43 and B replaced by w. The effective area and column strength are calculated as,

$$A_e = \sum b_e t + A_c \tag{27}$$

$$P_n = A_e F_n. \tag{28}$$

where A_c is the corner area.

Bending

a) The flexural-torsional buckling moment for an equal angle subjected to uniform bending with compression at the free edge of the flanges, as shown in Fig. 3a, is given by

$$M_n = S_c F_c \tag{29}$$

where S_c is the elastic section modulus of the effective cross-section corresponding to bending, and F_c is the inelastic flexural-torsional buckling stress determined as

$$F_c = \begin{cases} F_y & \text{for } \lambda_b \le 0.6 \\ 1.11\left[1-\left(\frac{10\lambda_b^2}{36}\right)\right]F_y & \text{for } 0.6 < \lambda_b \le 1.336 \\ \frac{F_y}{\lambda_b^2} & \text{for } \lambda_b > 1.336 \end{cases} \tag{30}$$

$$\lambda_b = \sqrt{\frac{F_y}{F_{eb}}}. \tag{31}$$

In eqn. (31), F_{eb} is the elastic buckling stress given by eqn. (15), which, for an equal angle in uniform bending with compression at the tips of the flanges, can be obtained from eqns (18,20), assuming sharp corners.

In determining the effective section modulus (S_c) of an equal angle bent in the plane of symmetry, the unstiffened flanges have tension at one edge and compression at the other. For such elements, the current provisions of the NAS Specification and AS/NZS4600 require the effective width to be calculated as if the elements were subject to uniform compression, *ie* using eqn. (13) with k=0.43.

b) When torsion is ignored, the bending strength is to be calculated as the section strength,

$$M_n = S_e F_y \tag{32}$$

where S_e is the section modulus of the effective cross-section calculated for the extreme tension or compression fibre at yield.

Combined compression and bending

A column is considered to be concentrically loaded if the line of action of the applied force (P) passes through the centroid of the effective cross-section, calculated at the buckling stress (F_n). In this case, the column strength is found using eqn. (28). If the load is applied with an eccentricity (e) relative to the effective centroid, the column shall be designed as a beam-column for the compression force (P) and a moment (M_y),

$$M_y = Pe. \tag{33}$$

It is common practice to measure the eccentricity of the force from the gross section centroid, in which case,

$$e = e_e + e_P \tag{34}$$

where e_e is the distance between the centroids of the gross and effective cross-sections, and e_P is the distance from the gross section centroid to the line of action of the applied force, as shown in Fig. 5. For slender angles, the NAS Specification and AS/NZS4600 require the member be designed for an additional eccentricity (e_L), ie

$$e = e_e + e_P + e_L \tag{35}$$

where

$$e_L = \frac{L}{1000}. \tag{36}$$

Since, generally, $e \neq 0$, a slender angle is required to be designed as a beam-column subjected to equal and opposite end moments (M_y), (uniform bending). Omitting resistance factors, the interaction equation is,

$$\frac{P}{P_n} + \frac{C_{my} M_y}{M_{ny} \alpha_y} \leq 1 \tag{37}$$

where $C_{my}=1$ for uniform bending. The amplification factor,

$$\alpha_y = 1 - \frac{P}{P_{E_y}}, \tag{38}$$

involves the Euler load for flexural buckling about the *y*-axis. Equations (33,37-38) lead to a quadratic equation for *P*.

3.2. New effective width equations for unstiffened elements under stress gradient

General

As mentioned in the previous section, the current provisions of the NAS Specification and AS/NZS4600 treat unstiffened elements under stress gradient as if subjected to uniform compression. Accordingly, the plate buckling coefficient is to be taken as $k=0.43$. This approach leads to conservative estimates of the effective width and hence, the section modulus of the effective cross-section in bending (S_c) and the bending strength (M_n) are conservatively predicted, as given by eqn. (29).

Based on recent research (Bambach and Rasmussen 2002b; a), effective width equations have been obtained for unstiffened elements subjected to in-plane bending. When applied to angles, the equations can be summarised as follows:

Compression at the unsupported edge

When bending causes a compressive stress (f_1) at the unsupported edge, as shown in Fig. 6a, the effective width is obtained using eqn. (24) with ρ given by,

$$\rho = \begin{cases} 1 & \text{for } \lambda_p \leq 0.673(1+\psi) \\ (1+\psi)(1-0.22(1+\psi)/\lambda_p)/\lambda_p & \text{for } \lambda_p > 0.673(1+\psi) \end{cases} \tag{39}$$

where λ_p is given by eqn. (26) with $f=f_1$ and F_{cr} determined using eqn. (13) with *B* replaced by *w* and *k* given by,

$$k = 0.57 + 0.21\psi + 0.07\psi^2. \tag{40}$$

In eqns (39,40), ψ is the numerical value of the stress ratio,

$$\psi = \left| \frac{f_2}{f_1} \right| \tag{41}$$

which is approximately unity for an equal angle in bending, ie k=0.85.

Compression at the supported edge

When bending causes a compression stress (f_1) at the supported edge, as shown in Fig. 6b, the effective width is obtained using eqn. (24) with ρ given by,

$$\begin{aligned} &\text{For } \psi < 1: \ \rho = \begin{cases} 1 & \text{for } \lambda_p \le 0.673(1+\psi) \\ (1-\psi)(1-0.22/\lambda_p)/\lambda_p + \psi & \text{for } \lambda_p > 0.673(1+\psi) \end{cases} \\ &\text{For } \psi \ge 1: \ \rho = 1 \end{aligned} \tag{42}$$

where ψ is given by eqn. (41), λ_p is given by eqn. (26) with f=f_1 and F_{cr} determined using eqn. (13) with B replaced by w and k given by,

$$k = 1.70 + 5\psi + 17.1\psi^2. \tag{43}$$

3.3. Shift of the effective centroid

According to the NAS Specification and AS/NZS4600, the eccentricity (e_e) arising from the shift of the effective centroid is to be calculated as the distance between the centroids of the gross and effective cross-sections. For an equal angle with sharp corners, this leads to the following expression,

$$e_e = (B - b_e)/(2\sqrt{2}) \tag{44}$$

where b_e is obtained from eqns (24-26) using k=0.43 in determining F_{cr}. It is here implicit that the line of action of the force in the locally buckled stated is assumed to be located at the centre of the effective width of the legs. However, while the effective width equations provide an accurate estimate of the strength of unstiffened elements, they do not accurately predict the location of the line of action of the force (Young and Rasmussen 1999). For an angle section, the shift of the effective centroid (e_e) is overestimated when using eqn. (44).

It is difficult to calculate the location of the internal force of a general cross-section because it involves the stress-distribution in the post-buckling range, which, in turn, requires a solution of the nonlinear von Karman equations. However, in the case of an equal angle in compression, the condition at the corner is exactly that of a simple support, and the stress distribution can therefore be found from Stowell's (Stowell 1949) classical solution. As shown in Appendix II, an accurate estimate of the shift of the effective centroid of an equal angle can be obtained as,

$$e_0 = \begin{cases} 0 & \text{for } \lambda_{py} \le 1.22 \\ \dfrac{5}{16\sqrt{2}} \dfrac{\lambda_{py} - 1.22}{\lambda_{py} - 0.22} & \text{for } \lambda_{py} > 1.22 \end{cases} \tag{45}$$

where λ_{py} is the plate slenderness calculated at the yield stress,

$$\lambda_{py} = \sqrt{\frac{F_y}{F_{cr}}}. \tag{46}$$

The shift of the effective centroid is denoted by e_0 in eqn. (45), as distinct from the eccentricity e_e which is based on the centroid of the effective cross-section.

4 Tests on equal angles with slender legs

4.1. Wilhoite et al. tests

Compression tests on equal angles with slender legs have been reported by Wilhoite et al. (1984) and Popovic et al. (1999). The tests are summarised as follows:

The angles tested by Wilhoite et al. (1984) were brake-pressed from high strength steel plates. The measured dimensions and measured value of yield stress for the flats (F_y) are shown in Table 1. Fixed-ended stub columns and three lengths of pin-ended long columns were tested. The lengths of the long columns were chosen so as to produce nominal L/r_y-values of 60, 90 and 120. The pin-ended columns were nominally loaded through the centroid of the gross cross-section. However, a small clearance was built into the pin-ended bearings to avoid locking, and an eccentricity of loading may have been induced as a result of this clearance. The bearings were manufactured to a tolerance that ensured the induced loading eccentricity would not exceed 1/1000 of the length of the longest columns. The test strengths and column lengths are shown in Table 2, as obtained from Fig. 18 of Wilhoite et al. (1984).

4.2. Popovic et al. tests

The angles tested by Popovic et al. (1999) were cold-rolled and in-line galvanised to produce a nominal yield stress value of 350 MPa. The measured dimensions and mechanical properties are shown in Table 1. Because of the cold-rolling, the yield stress varied across the cross-section with the highest values obtained at the corners. The measured yield stress value shown in Table 1 was obtained from the middle of the flat part of the legs.

Seven fixed-ended columns and ten pin-ended columns were tested. The L_e/r_y-values ranged from 7 to 130 and from 46 to 130 for the fixed-ended and pin-ended tests respectively. For the pin-ended columns, the effective length (L_e) is the sum of the specimen length and the total lengthwise dimension of the end bearings. The effective length (L_e) is taken as half of the specimen length for the fixed-ended specimens. The use of an effective length of half of the specimen length accounts correctly for the effect of fixed ends at long lengths, at which the column fails by minor axis flexural buckling. However, it is less meaningful to use an effective length of half of the specimen length at short lengths because the critical overall mode becomes the flexural-torsional mode, for which the torsional component is independent of the length.

The pin-ended columns were loaded with a nominal eccentricity of 1/1000 of the column length relative to the gross section centroid. Two tests were performed at each length, one where the load was applied eccentrically towards the free edges of the flanges (causing increased compression at the free edges), and one where the load was applied eccentrically towards the corner. Consistently, the lowest test strength was obtained when the eccentricity caused increased compression at the free edges. The geometric imperfections were measured

on all specimens, as detailed in Popovic et al. (1996), indicating an average overall minor axis flexural imperfection of $L/1305$. The test strengths and column lengths are shown in Table 3.

The loading eccentricity was introduced in the tests not for the purpose of investigating the effect of a loading eccentricity but to account for the effect of overall geometric imperfections of a magnitude of a thousandth of the length. Accordingly, in the comparison with design loads, the columns are treated as loaded through the gross section centroid.

5 Proposed design procedure for angles with slender legs

5.1. Equal angles

General design approach

In the following development of a suitable design model for angles with slender legs, the focus is on the torsional buckling mode, the effective width calculation of angles in bending and the eccentricity required to account for the effect of the shift in the effective centroid. The design strength calculations are based on the measured cross-section dimensions and mechanical properties given in Table 1, and account for the roundedness of the corners.

The design strength obtained using the current provisions of the NAS Specification and AS/NZS4600 are compared with the test results detailed in Tables 2 and 3 in Figs 7a and 7b for the Wilhoite et al. and Popovic et al. angles respectively. The design strength is shown as the P_1 curve in both figures. It considers the minor axis flexural and the flexural-torsional buckling modes in calculating the elastic column buckling stress $F_e=\min\{\sigma_{ey}, F_{ext}\}$, and determines the bending strength (M_n) based on the flexural-torsional buckling capacity according to eqns (29-31). The section modulus (S_e) is based on an effective section calculated using k=0.43. Since the columns were treated as loaded through the gross section centroid (e_P=0), the eccentricity is calculated according to eqn. (35) as e_e+e_L where e_e is the distance between the centroids of the gross and effective cross-sections. These main features of the design model are summarised in Table 4.

It follows from Figs 7a and 7b that the design strengths (P_1) are significantly lower than the test strengths at short and intermediate lengths. The reason is partly that the torsional (local) buckling mode is accounted for in determining the P_n and M_n capacities, as well as in determining the effective area (A_e), as mentioned in the Introduction. It could be considered to account for the torsional mode in calculating P_n and M_n and then using the full area rather the effective area. However, this approach would lead to conservative strengths at short lengths, since it would not incorporate the post-local buckling strength of unstiffened elements. A more efficient approach is therefore to ignore the torsional mode in determining P_n and M_n, and to use the effective area in calculating P_n. This implies that the elastic buckling stress (F_e) shall be taken as the minor axis flexural buckling stress (σ_{ey}), and the bending capacity becomes the section capacity determined according to eqn. (32). All design models investigated here onwards will be based on this approach.

The new design models (P_2, P_3,…, P_9) are defined in Table 4. The main features of the P_2-P_5 models are that a) they ignore torsional buckling in determining the buckling strength (P_n) and the bending capacity (M_n), and b) the section modulus (S_e) is based on effective widths determined using a buckling coefficient of k=0.43, which is the current conservative approach of the NAS Specification and AS/NZS4600 for unstiffened elements under stress gradient. Various loading eccentricities (e) are considered, including $e = e_e+e_L$, $e = e_e$, $e = e_L$ and $e = 0$.

The design strengths are compared with the Wilhoite et al. and Popovic et al. test strengths in Figs 7a and 7b respectively.

The design model P_2 is the same as P_1 except that torsional buckling is ignored in determining P_n and M_n. It can be seen from Figs 7a and 7b that a *lower* strength curve in fact results from ignoring torsion, which is because even though the axial capacity (P_n) is substantially enhanced, the shift of the effective centroid (e_e) is also increased, as it is calculated at the enhanced buckling stress, and the combined effect is such that the interaction equation (37) leads to a slightly lower value of P. If the additional eccentricity ($e_L = L/1000$) is omitted (P_3), (e_L is the additional eccentricity imposed on slender angles in the NAS Specification and AS/NZS4600), the strength curve is raised in the intermediate length range and is slightly above one of the Popovic et al. test points at an L/r_y-value of 129. The strength curve drops initially with decreasing length where it branches off the column strength curve (P_5) and becomes increasingly conservative at short lengths compared with the test results. The P_3 strength curve branches off the column strength curve when the section become non-fully effective, which occurs at L/r_y-values of 148 and 140 for the Wilhoite et al. and Popovic et al. angles respectively. As the length decreases from these points, the effect of the shift of the effective centroid (e_e) is greater than the increase in axial capacity (P_n) and the strength initially decreases as the length decreases. If the eccentricity is taken as e_L (P_4), *ie* the effect of the shift in the effective centroid is accounted for by virtue of e_L rather than e_e, the strength curve is significantly increased and, in fact, provides an accurate estimate of the test strengths. However, the agreement is coincidental, since it is a result of a very conservative estimate of the bending capacity (M_n) based on k=0.43 which compensates for the fact that the eccentricity (e_L) underestimates the effect of the shift of the effective centroid at short lengths where $e_L \rightarrow 0$. If the columns were designed as concentrically loaded struts (P_5), the strength curve is clearly higher than the test strengths, thus emphasising that the effect of the shift in the effective centroid needs to be accounted for.

Figures 8a and 8b show similar comparisons to those shown in Figs 7a and 7b except that the section modulus of the effective section in bending (S_e) is based on the accurate effective width equations (39,40), by which the Wilhoite et al. and Popovic et al. test sections become fully effective in bending. The design models are denoted by P_6-P_9 and defined in Table 4. It follows that $P_6 \sim P_2$, $P_7 \sim P_3$ and $P_8 \sim P_4$, except for the difference in M_n, while P_9 is based on the accurate calculation of the shift in the effective centroid (e_0) given by eqn. (45). A sample calculation of the P_9 design strength for one of the angle columns tested by Wilhoite et al. is included in Appendix III. It follows from Figs 8a and 8b that the P_6 and P_7 strength curves are significantly higher than their P_2 and P_3 counterparts but remain conservative because the shift of the effective centroid (e_e) is overestimated. The design model P_8 now becomes optimistic for a large number of test points because the eccentricity (e_L) underestimates the effect of the shift in the effective centroid. However, excellent agreement with the Popovic et al. test results is achieved when the eccentricity (e_0) is based on the accurate expression (45). The Wilhoite et al. test results are reasonably accurately predicted, albeit conservatively at intermediate lengths. This result shows that the interaction equation (37) can accurately predict the strength of equal angles with slender legs provided the torsional mode is ignored in determining P_n and M_n, the accurate effective width equations (39,40) are used for determining M_n and the shift of the effective centroid (e_0) is calculated using eqn. (45). Equal angle columns with slender legs can thus be designed using a beam-column approach with the eccentricity calculated as,

$$e = e_0 + e_P \tag{47}$$

where e_0 is calculated according to eqn. (45) and the loading eccentricity (e_P) is measured from the centroid of the gross cross-section, as shown in Fig. 5. It is not necessary to include the additional eccentricity $e_L=L/1000$ currently specified in the American and Australian standards.

As shown in Fig. 8b, the design model P_9 also produces accurate strength predictions for the Popovic et al. fixed-ended tests, except at short lengths where the tests strengths are significantly higher than the design curve because the shift in the effective centroid does not induce overall bending in fixed-ended columns (Rasmussen and Hancock 1993). In fact, it could have been expected that the fixed-ended test points would lie close to the P_5 pure column design curve. However, the P_5 curve has been calibrated for columns failing by flexural buckling while slender angle section columns fail by flexural-torsional buckling at short and intermediate lengths. Furthermore, it is not clear whether the effective length concept is readily applicable to columns failing primarily by torsion at short lengths. The comparison shown in Fig. 8b demonstrates that fixed-ended slender angle section columns cannot simply be designed as concentrically loaded columns using the strength curve for flexural buckling. The design model P_9 works well for the Popovic et al. section but becomes conservative for fixed-ended equal angle columns with more slender cross-sections.

Design approach for concentrically loaded columns

While an accurate design model thus has been achieved, which is in line with the NAS Specification and AS/NZS4600, the model leads to a relative involved beam-column design calculation for the common case where the load is applied at the centroid of the gross cross-section ($e_P=0$). It is possible to obtain a more direct column design approach for this case, as follows:

In the limit $L\rightarrow 0$, the interaction equation (37) for a column loaded through the gross section centroid reduces to,

$$\frac{P}{P_{n0}}+\frac{e_0 P}{M_n}\leq 1 \tag{48}$$

where $P_{n0}=A_e F_y$ with A_e based on F_y. Thus,

$$P_{n0,r}=\beta P_{n0} \tag{49}$$

where the reduction factor β,

$$\beta=\frac{1}{1+\frac{e_0 P_{n0}}{M_n}}, \tag{50}$$

accounts for the effect of the shift of the effective centroid at short lengths ($L\rightarrow 0$). For an equal angle with sharp corners, expressions are readily derived for P_{n0} and M_n in terms of λ_{py}. Combining these with eqn. (45), the following expression is obtained

$$\beta = \begin{cases} 1 & \text{for } \lambda_{py} \le 1.22 \\ \dfrac{1}{1+\frac{15}{8}(\lambda_{py}-1.22)/\lambda_{py}^2} & \text{for } 1.22 < \lambda_{py} \le 0.673(1+\psi)/r_k \\ \dfrac{1}{1+\frac{15}{8}(\lambda_{py}-1.22)r_k^2/\left[(1+\psi)^2(1-0.22\frac{1+\psi}{r_k\lambda_{py}})^2\right]} & \text{for } \lambda_{py} > 0.673(1+\psi)/r_k \end{cases} \quad (51)$$

where λ_{py} is calculated from eqn. (46) using F_y and k=0.43, and

$$r_k = \sqrt{\frac{k_c}{k_b}} \quad (52)$$

with k_c=0.43 and k_b given by eqn. (40). For an equal angle with sharp corners, ψ=1 $\Rightarrow$ k_b=0.85 $\Rightarrow$ r_k=0.711, and thus

$$\beta = \begin{cases} 1 & \text{for } \lambda_{py} \le 1.22 \\ \dfrac{1}{1+1.875(\lambda_{py}-1.22)/\lambda_{py}^2} & \text{for } 1.22 < \lambda_{py} \le 1.89 \\ \dfrac{1}{1+0.237(\lambda_{py}-1.22)/(1-\frac{0.619}{\lambda_{py}})^2} & \text{for } \lambda_{py} > 1.89 \end{cases} \quad (53)$$

Figure 9 shows a plot of β *vs* λ where the expressions given in eqn. (53) are shown dashed outside their validity ranges. A slightly conservative approximation to eqn. (53) can be obtained as

$$\beta = \begin{cases} 1 & \text{for } \lambda_{py} \le 1.22 \\ \dfrac{0.68}{(\lambda_{py}-1)^{\frac{1}{4}}} & \text{for } \lambda_{py} > 1.22 \end{cases}, \quad (54)$$

as also shown in Fig. 9.

Equation (49) predicts the capacity of a short length of an equal angle loaded through the gross section centroid. A simple column design procedure can now be obtained by assuming that the reduction factor (β) applies over the full range of lengths, *ie*

$$P_{n,r} = \beta P_n \quad (55)$$

where β is given by eqn. (54) and $P_n = F_n A_e$ is obtained using eqn. (21) with A_e based on the buckling stress F_n. A sample calculation of the $P_{n,r}$ design strength for one of the angle

columns tested by Wilhoite et al. is included in Appendix III. The design strength ($P_{n,r}$) is compared with the Wilhoite et al. and Popovic et al. tests in Figs 10a and 10b respectively. The figure also includes the design strength P_9, which is based on a beam-column design approach with $e=e_0$. It follows from the figures that the column design strength $P_{n,r}$ is in close agreement with the P_9 design model and is in good agreement with the test strengths.

5.2. Unequal angles

The agreement demonstrated in the previous section between the design model P_9 and the Wilhoite et al. and Popovic et al. test strengths can be attributed to the fact that it is based on accurate expressions for a) the column strength (P_n), b) the shift of the effective centroid (e_0), and c) the effective widths for calculating the section capacity (M_n). These expressions can be expected to work equally well for unequal angles, and so the following design approach is proposed:

The strength of an unequal angle column loaded with eccentricities e_{Px} and e_{Py} in the directions of the principal x and y axes respectively, as shown in Fig. 11, shall be determined using the interaction equation,

$$\frac{P}{P_n}+\frac{C_{my}M_y}{M_{ny}\alpha_y}+\frac{C_{mx}M_x}{M_{nx}\alpha_x}\le 1 \tag{56}$$

where, $C_{mx}=C_{my}=1$ since the eccentric loading causes uniform bending about both principal axes, $\alpha_y=1-P/P_{Ey}$ and $\alpha_x=1-P/P_{Ex}$ are amplification factors, P_n is the column capacity determined on the basis of $F_e=\min\{\sigma_{ey}, \sigma_{ex}\}$ (*ie* ignoring torsion), $M_{ny}=S_{ey}F_y$ and $M_{nx}=S_{ex}F_y$ are the section capacities for bending about the y and x-axes respectively, where the effective widths of the legs shall be determined using eqns (39-43), and the moments M_y and M_x are given by,

$$M_y=(e_{0x}+e_{Px})P \tag{57}$$

$$M_x=(e_{0y}+e_{Py})P \tag{58}$$

The shifts of the effective centroid in the principal axis directions (e_{0y},e_{0x}) can be calculated according to the expressions derived in Appendix II as,

$$e_{0x}=\frac{1}{1+\gamma}\left[s_B\sin\alpha+\gamma s_D\cos\alpha\right] \tag{59}$$

$$e_{0y}=\frac{1}{1+\gamma}\left[s_B\cos\alpha-\gamma s_D\sin\alpha\right] \tag{60}$$

where α is the rotation of the principal axis relative to the legs, as shown in Fig. 11, γ is the ratio between the flat widths of the narrow and wide legs,

$$\gamma=\frac{d}{b}, \tag{61}$$

and the shifts parallel to the legs (s_B,s_D) are given by,

$$s_B = \begin{cases} 0 & \text{for } \lambda_{py,b} \le 1.22 \\ \frac{5}{16}\dfrac{\lambda_{py,b} - 1.22}{\lambda_{py,b} - 0.22} B & \text{for } \lambda_{py,b} > 1.22 \end{cases} \quad (62)$$

$$s_D = \begin{cases} 0 & \text{for } \lambda_{py,b} \le 0.22 + 1/\gamma^2 \\ \frac{5}{16}\dfrac{\lambda_{py,b} - (0.22 + 1/\gamma^2)}{\lambda_{py,b} - 0.22} \gamma B & \text{for } \lambda_{py,b} > 0.22 + 1/\gamma^2 \end{cases} \quad (63)$$

In eqns (62,63), $\lambda_{py,b}$ is the plate slenderness of the leg with flat width b calculated at the yield stress.

For an unequal angle, the angle (α) is given by

$$\alpha = \tfrac{1}{2}\tan^{-1}\left(\frac{6\gamma^2}{-\gamma^4 - 4\gamma^3 + 4\gamma + 1}\right), \quad \gamma \le 1 \quad (64)$$

For $0.5 \le \gamma \le 1$, this expression can be approximated closely by

$$\alpha \approx 1.05\gamma - 0.2625, \quad 0.5 \le \gamma \le 1, \quad (65)$$

where α is in radian.

6 Conclusions

A detailed study has been reported of the elastic local, flexural, torsional and flexural-torsional buckling modes of slender equal angle sections, including their interdependency. Various design models have been compared with tests by systematically changing the choice of critical overall buckling mode, the effective width equation, and the loading eccentricity. It is shown that an accurate design model can be achieved by:

a) ignoring torsional buckling in determining the compression and bending member strengths,
b) adopting recently reported effective width equations for unstiffened elements under stress gradient, and
c) determining the shift of the effective centroid from a simple expression that is based on the actual post-buckling stress distribution.

The design model has been shown to be in good agreement with tests on pin-ended slender equal angle columns loaded through the gross section centroid or with a small eccentricity from the gross section centroid. The design model is also show to provide accurate strength predictions for fix-ended slender angle columns, except at short lengths where the design strength prediction becomes conservative.

The report focuses on slender equal angle section columns loaded concentrically or eccentrically relative to the gross section centroid. The proposed accurate design model is based on a beam-column approach and requires calculation of the axial and bending capacities. A simple design model is proposed for the common case where the column is concentrically loaded through the gross section centroid. The model applies a reduction factor

to the pure column design strength and does not require calculation of the bending capacity nor the use of an interaction equation.

Based on the study of equal angles, a beam-column model is proposed for the design of slender unequal angle columns. Equations are provided for determining the shift of the effective centroid in the directions of the principal axes based on the actual post-buckling stress distribution. The legs are assumed not to interact in determining the local and post-local buckling stress.

7 Acknowledgements

This report was prepared while the author was on study leave at the University of Trento. The facilities provided by the University of Trento are gratefully appreciated. Thanks also to Professor Gregory Hancock for his comments to this manuscript.

Tables

Table 1: Geometric and material properties of the Wilhoite et al. and Popovic et al. cross-sections

Section	B	t	r_i	A	I_x	I_y	J	x_0	F_y	E
	mm	mm	mm	mm^2	mm^4	mm^4	mm^4	mm	MPa	MPa
Wilhoite et al.	69.3	3.00	3.0	401	311200	74150	1203	24.2	465	203000
Popovic et al.	50.8	2.30	2.6	224	93830	22150	396	17.7	396	203000

Table 2: Test strengths reported by (Wilhoite et al. 1984); P_y=186kN, r_y=13.6mm

Test	L_e	L_e/r_y	P_u	P_u/P_y
	mm		kN	
1	823	60.5	72.5	0.388
2	1227	90.2	58.3	0.312
3	1227	90.2	60.1	0.322
4	1227	90.2	65.0	0.348
5	1636	120.2	48.4	0.259
6	1636	120.2	52.1	0.279
7	1636	120.2	59.2	0.317

Table 3: Test strengths reported by (Popovic et al. 1999); P_y=88.7kN, r_y=9.94mm

	Test	L^*_e	L_e/r_y	P_u	P_u/P_y
		mm		kN	
Pin-ended tests	1	459	46.2	41.7	0.466
	2	458	46.1	47.2	0.528
	3	676	68.0	35.2	0.394
	4	676	68.0	40.1	0.448
	5	862	86.7	30.9	0.345
	6	863	86.8	47.5	0.531
	7	1088	109.5	25.1	0.280
	8	1088	109.5	32.1	0.359
	9	1285	129.3	17.7	0.198
	10	1286	129.4	24.7	0.276
Fixed-ended tests	1	75	7.5	71.4	0.798
	2	275	27.7	54.0	0.604
	3	485	48.8	41.5	0.464
	4	690	69.4	37.0	0.414
	5	874	87.9	31.3	0.350
	6	1100	110.6	26.4	0.295
	7	1299	130.7	22.3	0.249

* L_e includes the end bearing dimensions for the pin-ended tests, and is half the specimen length for the fixed-ended tests

Table 4: Summary of design models

	Compression	Bending		
Design model	F_e	M_n	e	b_e
P_1*	$\min\{\sigma_{ey},F_{0xt}\}$	S_cF_c	e_e+e_L	k=0.43
P_2	σ_{ey}	S_eF_y	e_e+e_L	k=0.43
P_3	σ_{ey}	S_eF_y	e_e	k=0.43
P_4	σ_{ey}	S_eF_y	e_L	k=0.43
P_5	σ_{ey}	S_eF_y	0	-
P_6	σ_{ey}	S_eF_y	e_e+e_L	k,ρ from eqns (39,40)
P_7	σ_{ey}	S_eF_y	e_e	k,ρ from eqns (39,40)
P_8	σ_{ey}	S_eF_y	e_L	k,ρ from eqns (39,40)
P_9	σ_{ey}	S_eF_y	e_0	k,ρ from eqns (39,40)

* Current NAS and AS/NZS4600 design model

Figures

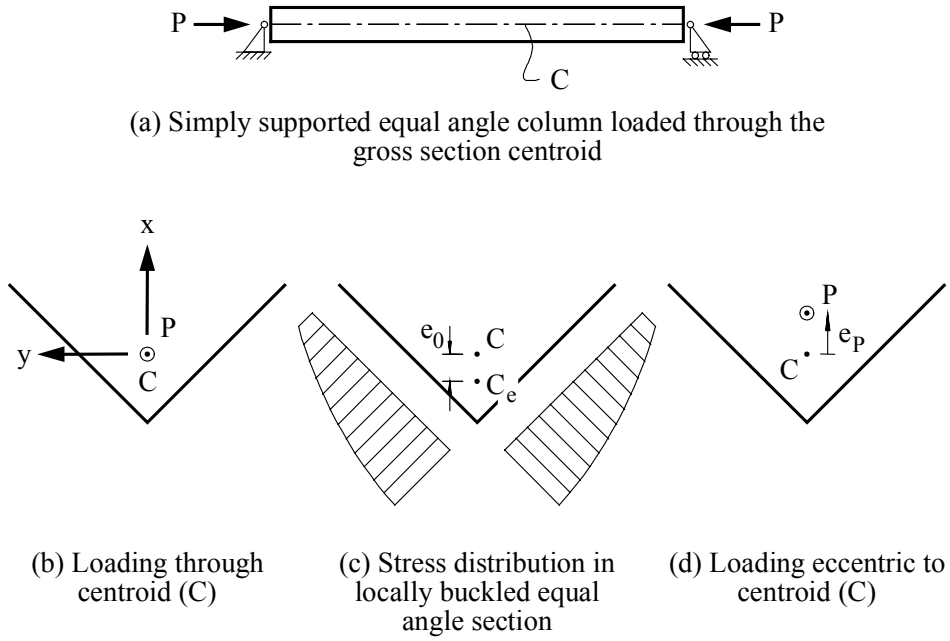

Figure 1: Simply supported angle column

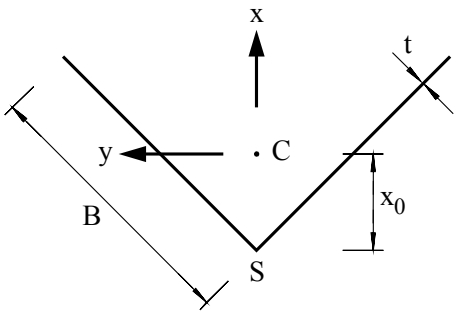

Figure 2: Nomenclature

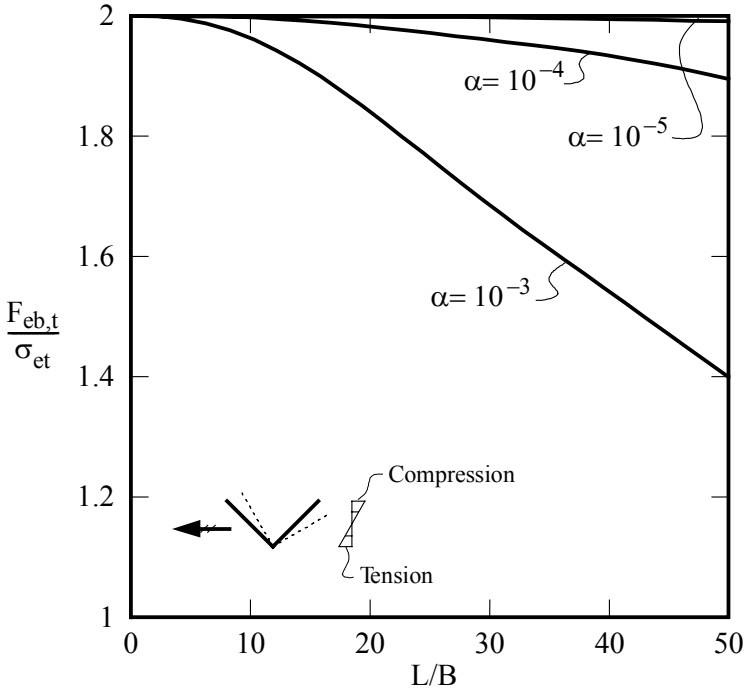

Figure 3a: Flexural-torsional buckling stress for bending causing compression at the flange tips

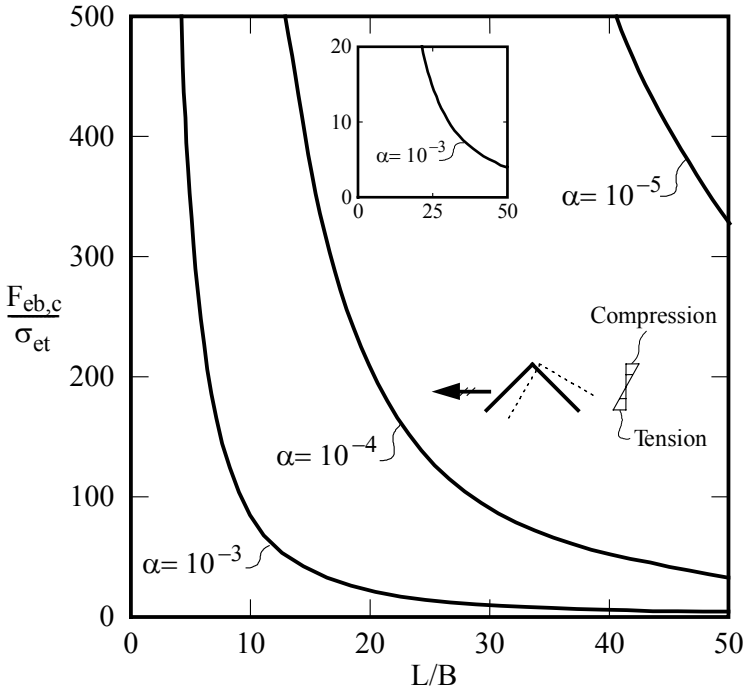

Figure 3b: Flexural-torsional buckling stress for bending causing compression at the flange junction

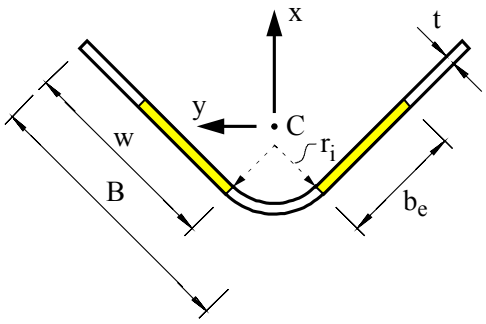

Figure 4: Flat and effective widths of cold-formed angle section

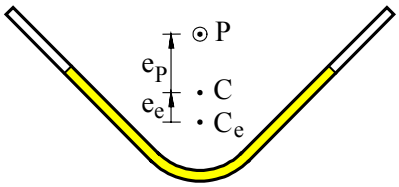

Figure 5: Eccentricities of loading of cold-formed angle section

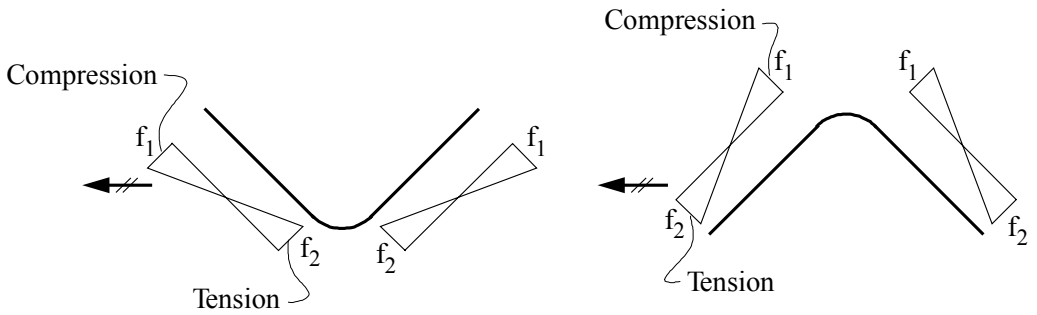

(a) Compression at the unsupported edge

(a) Compression at the supported edge

Figure 6: Definition of design stresses (f_1,f_2)

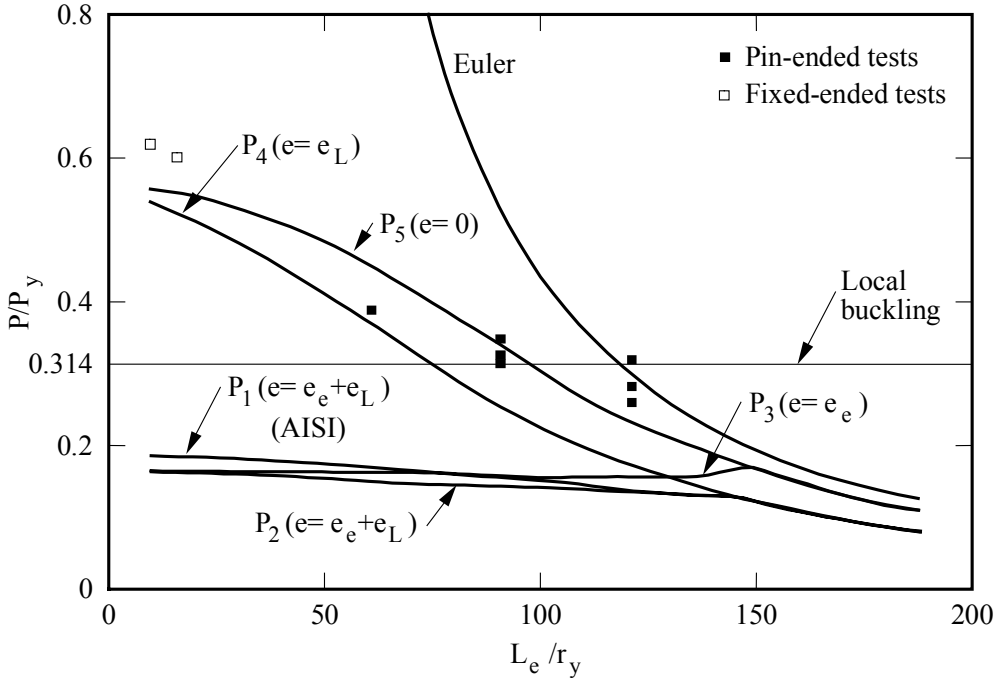

Figure 7a: Comparison of design strengths (P_1 - P_5) with tests on the Wilhoite et al. equal angle section

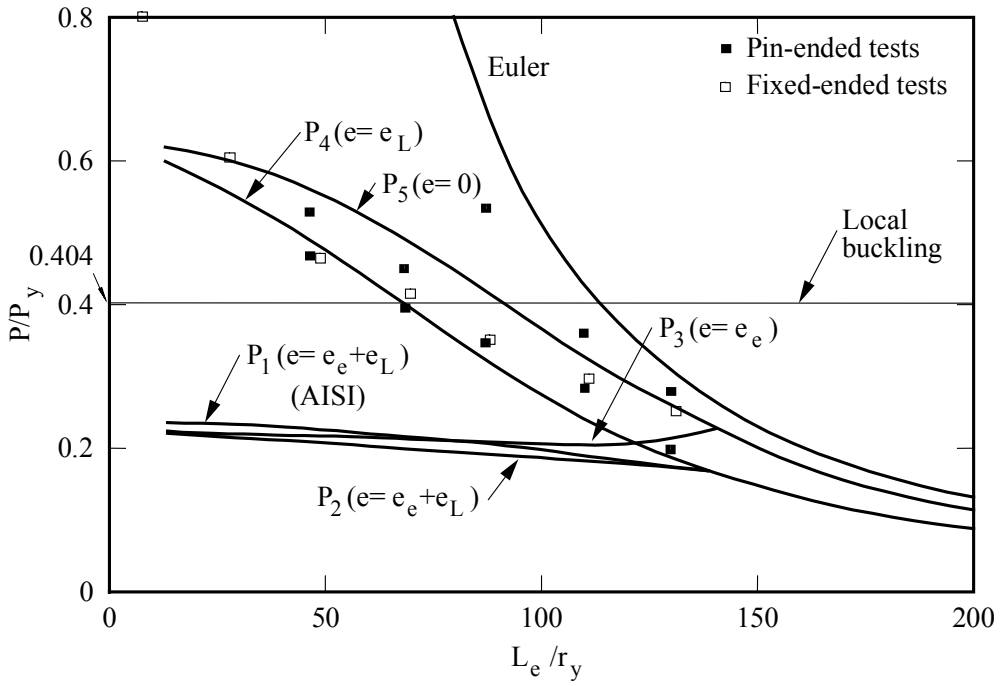

Figure 7b: Comparison of design strengths (P_1 - P_5) with tests on the Popovic et al. equal angle section

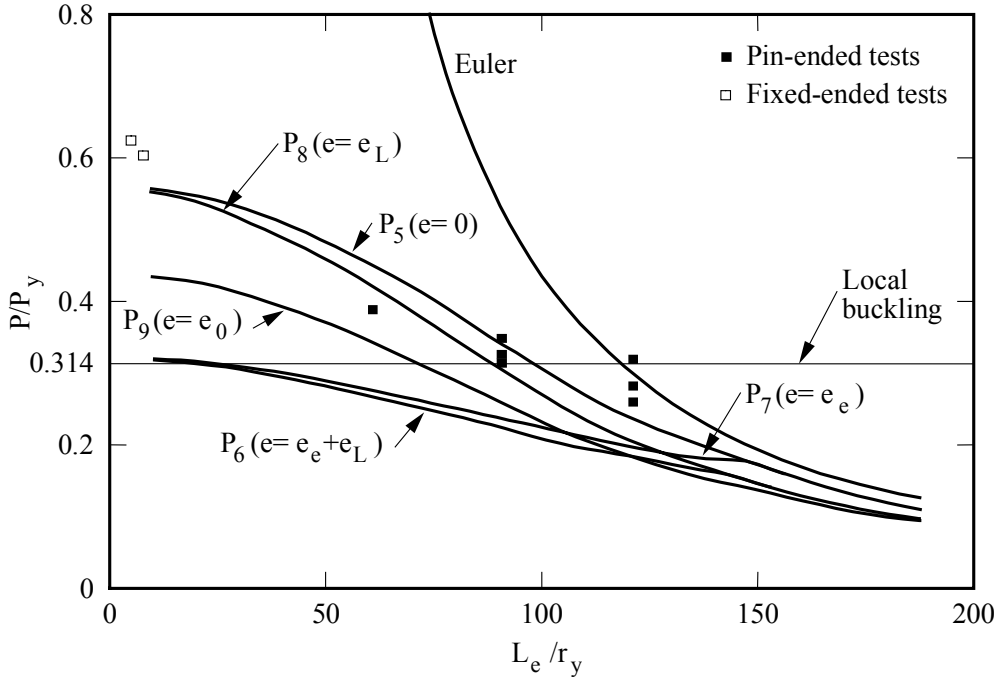

Figure 8a: Comparison of design strengths (P_5 - P_9) with tests on the Wilhoite et al. equal angle section

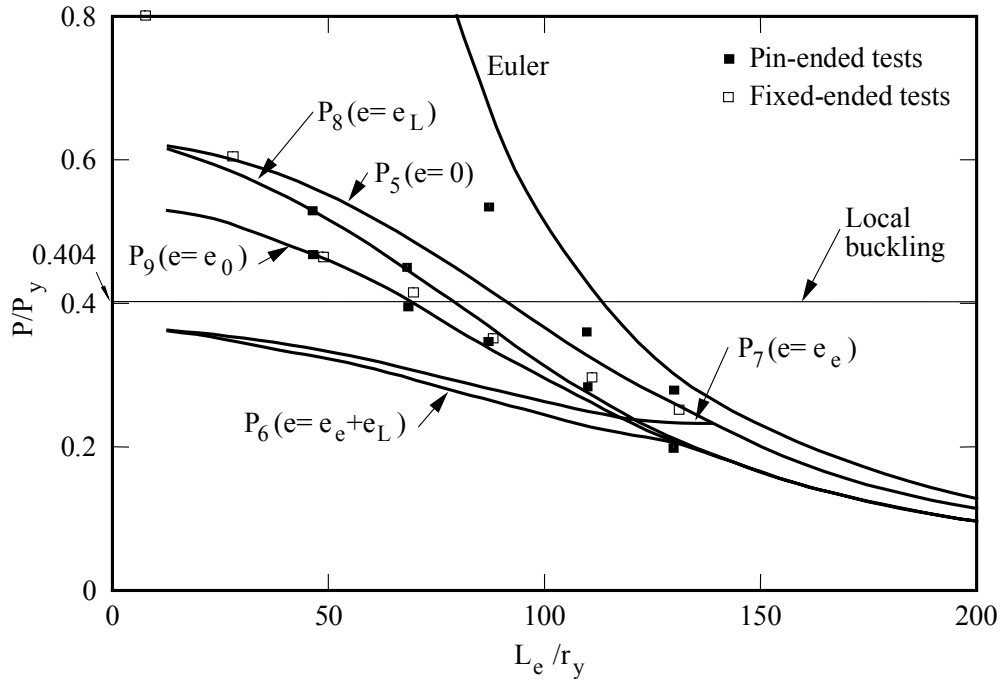

Figure 8b: Comparison of design strengths (P_5 - P_9) with tests on the Popovic et al. equal angle section

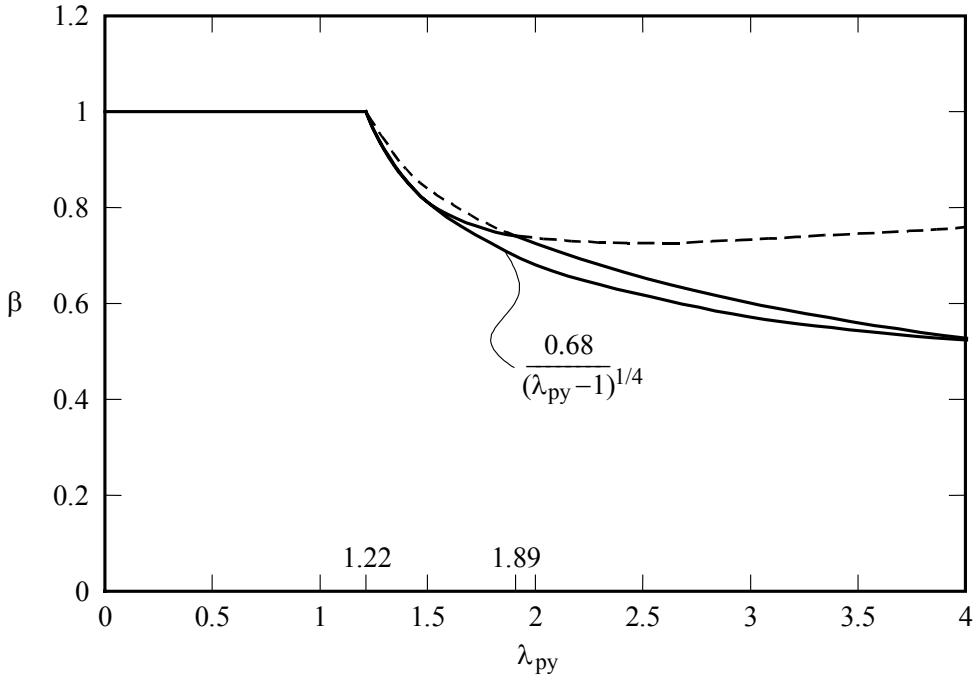

Figure 9: Exact and approximate expressions for β vs λ_{py}

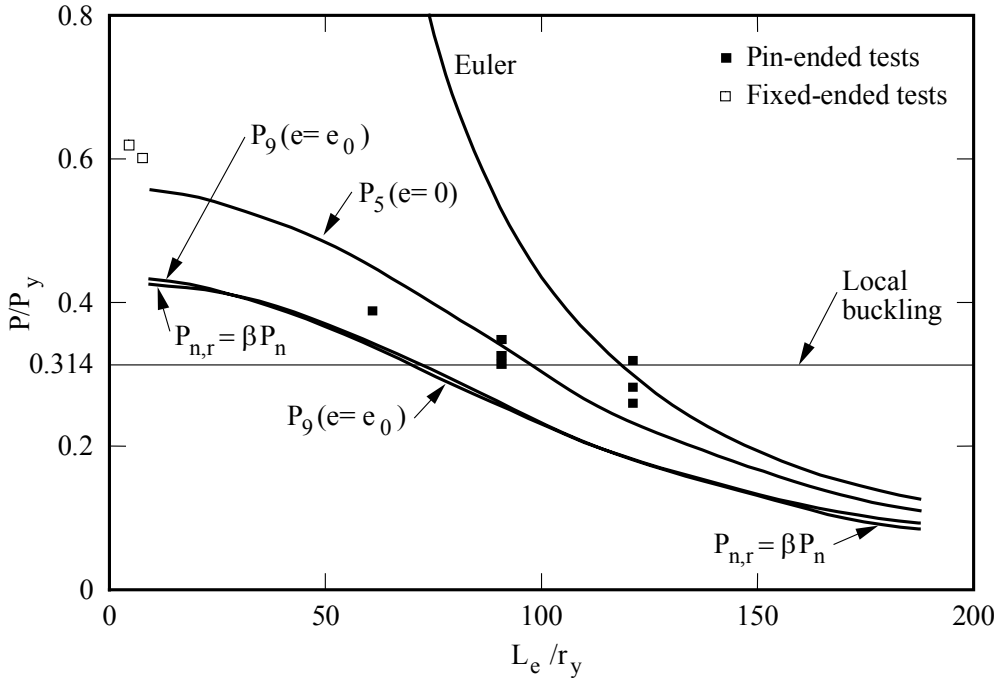

Figure 10a: Comparison of column design strength ($P_{n,r}=\beta P_n$) with tests on the Wilhoite et al. equal angle section

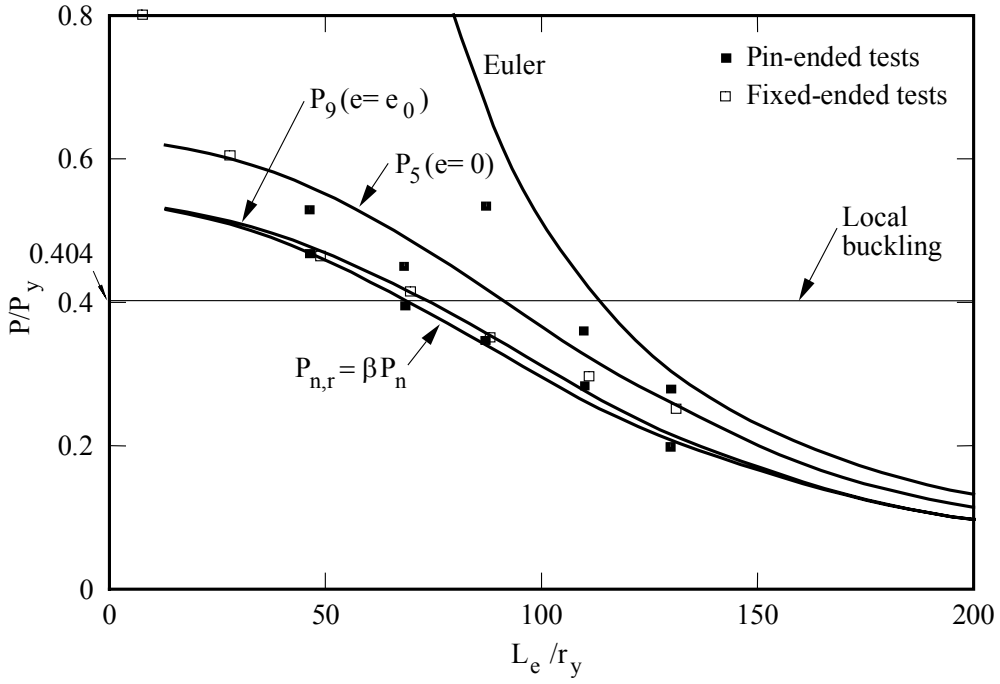

Figure 10b: Comparison of column design strength ($P_{n,r}=\beta P_n$) with tests on the Popovic et al. equal angle section

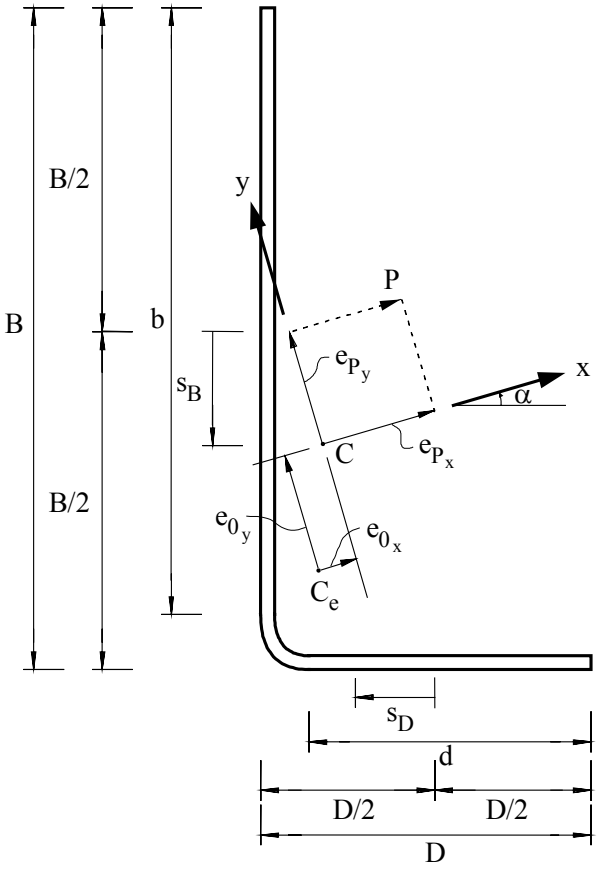

Figure 11: Nomenclature for unequal angle section

Appendix I: References

AS/NZS4600 (1996). Cold-formed Structures, AS/NZS 4600, Standards Australia, Sydney.

Bambach MR and Rasmussen, KJR (2002a). Elastic and Plastic Effective Width Equations for Unstiffened Elements. *Research Report R819*, Department of Civil Engineering, University of Sydney.

Bambach MR and Rasmussen, KJR (2002b). Tests on Unstiffened Elements under Bending and Compression. *Research Report R818*, Department of Civil Engineering, University of Sydney.

Bulson PS (1969). *The Stability of Flat Plates*. New York, Elsevier.

Chajes A and Winter, G (1965). "Torsional-flexural Buckling of Thin-walled Members." *Journal of the Structural Division, American Society of Civil Engineers* **91**(8).

NAS (2000). North American Specification for the Load and Resistance Factor Design of Cold-formed Steel Structural Members, American Iron and Steel Institute, Washington.

Popovic D, Hancock, GJ and Rasmussen, KJR (1996). Axial Compression Tests of Duragal Angles. *Research Report R730*, Department of Civil Engineering, University of Sydney.

Popovic D, Hancock, GJ and Rasmussen, KJR (1999). "Axial Compression Tests of Cold-formed Angles." *Journal of Structural Engineering, American Society of Engineers* **125**(5): 515-523.

Rasmussen KJR and Hancock, GJ (1993). "The Flexural Behaviour of Fixed-ended Channel Section Columns." *Thin-walled Structures* **17**(1): 45-63.

Rhodes J and Harvey, JM (1977). Interaction Behaviour of Plain Channel Columns under Concentric or Eccentric Loading. Second International Colloquium on the Stability of Steel Structures, ECCS, Liege**:** 439-444.

Stowell EZ (1949). Compressive Strength of Flanges. *Technical Note No. 1556*, National Advisory Committee for Aeronautics.

Timoshenko SP (1945). Theory of Bending, Torsion and Buckling of Thin-walled Members of Open Cross section, Journal of the Franklin Institute.

Wilhoite G, Zandonini, R and Zavelani, A (1984). Behaviour and Strength of Angles in Compression: An Experimental Investigation. ASCE Annual Convention and Structures Congress, San Francisco.

Young B and Rasmussen, KJR (1999). "Shift of Effective Centroid of Channel Columns." *Journal of Structural Engineering, American Society of Engineers* **125**(5): 524-531.

Appendix II. Derivation of equation to determine the shift in the effective centroid of equal and unequal angles

II.1 Equal angles

According to Stowell (1949), the post-buckling longitudinal strain (ε_x) of an unstiffened plate is approximately given by,

$$\varepsilon_x = \varepsilon_{av} + \frac{5}{4}(\varepsilon_{av} - \varepsilon_{cr})(1 - 3\left(\frac{y}{B}\right)^2) \qquad \text{(II.1)}$$

where (ε_{av}) and (ε_{cr}) are the average and critical strain respectively, and *y* is the transverse coordinate, as shown in Fig. II.1.

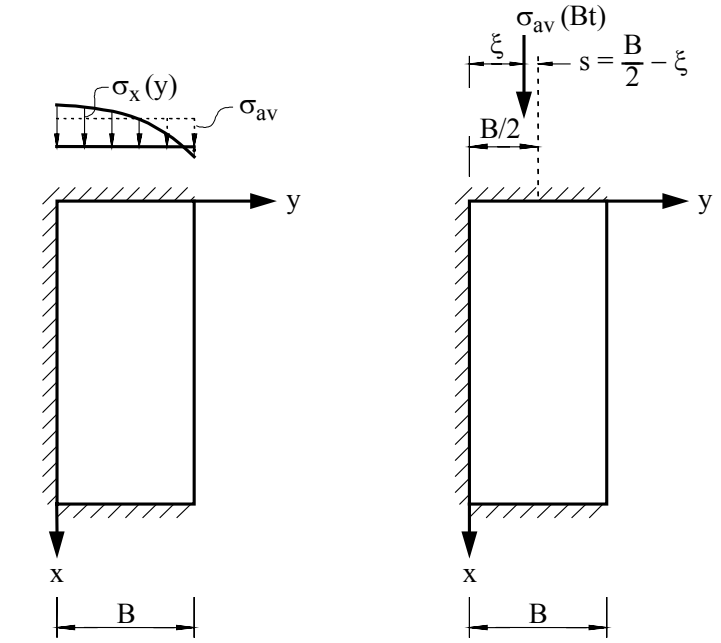

(a) Stress distribution (b) Resultant force

Figure II.1: Stress distribution and resultant force in a locally buckled unstiffened element

In the elastic range, Stowell's analysis is premised on a linear relationship between stress and strain, $\sigma_x = E\varepsilon_x$, and hence, the longitudinal stress is

$$\sigma_x = \sigma_{av} + \frac{5}{4}(\sigma_{av} - \sigma_{cr})(1 - 3\left(\frac{y}{B}\right)^2) \qquad \text{(II.2)}$$

where (σ_{av}) and (σ_{cr}) are the average and critical stress respectively.

The resultant force acting on the plate is σ_{av}(Bt). The line of action (ξ) of the force can be determined by taking moment about the supported longitudinal edge,

$$\sigma_{av} Bt\xi = \int_0^B \sigma_x yt\, dy \qquad \text{(II.3)}$$

By substituting eqn. (II.2) into eqn. (II.3) and carrying out the integration, ξ is determined as,

$$\xi = \tfrac{1}{2}B - \tfrac{5}{16}(1 - \frac{\sigma_{cr}}{\sigma_{av}})B \qquad \text{(II.4)}$$

The shift in the line of action of the force (s=B/2-ξ) is then (see Fig. II.1),

$$s = \tfrac{5}{16}(1-\frac{\sigma_{cr}}{\sigma_{av}})B = \tfrac{5}{16}(1-\frac{\sigma_{cr}}{\sigma_y}\frac{\sigma_y}{\sigma_{av}})B \qquad \text{(II.5)}$$

Denoting the plate slenderness calculated at the yield stress by λ_y and assuming the average stress at the ultimate load can be approximated by the Winter equation we have,

$$\frac{\sigma_{cr}}{\sigma_y} = \frac{1}{\lambda_y^2} \qquad \text{(II.6)}$$

$$\frac{\sigma_y}{\sigma_{av}} = \frac{1}{\rho} = \frac{1}{(1-0.22/\lambda_y)/\lambda_y} \qquad \text{(II.7)}$$

Substituting eqns (II.6,II.7) into eqn. (II.5), the shift in the line of action of the force is obtained as,

$$s = \tfrac{5}{16}\frac{\lambda_y - 1.22}{\lambda_y - 0.22}B \qquad \text{(II.8)}$$

This expression is valid for λ_y>1.22.

The shift in the effective centroid (CC_e) of an equal angle (see Fig.II.2) can now be obtained as,

$$e_0 = s/\sqrt{2} = \frac{5}{16\sqrt{2}}\frac{\lambda_y - 1.22}{\lambda_y - 0.22}B \qquad \text{(II.9)}$$

For equal angles with rounded corners (r_i≠0), this expression for e is associated with a small error.

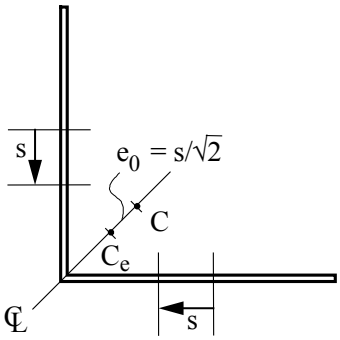

Figure II.2: Shift of line of action of the force in an equal angle section

II.2 Unequal angles

The expression for e_0 derived in Section II.1 can also be used for determining the location of the internal force of an unequal angle, provided the following assumptions are made:

1. The legs are assumed not to interact their junction. This implies that they have different elastic buckling stresses.
2. The ultimate strength of the section is determined as the Winter ultimate stress of the most slender leg.

Denoting the width of the wide and narrow legs by B and D, respectively, and introducing the ratio between the widths,

$$\gamma = \frac{D}{B}, \tag{II.10}$$

the shift of the resultant forces of each of the two legs (see Fig. II.3a) are given by,

$$s_B = \tfrac{5}{16}(1 - \frac{\sigma_{cr,B}}{\sigma_y}\frac{\sigma_y}{\sigma_{av}})B \tag{II.11}$$

$$\begin{aligned} s_D &= \tfrac{5}{16}(1 - \frac{\sigma_{cr,D}}{\sigma_y}\frac{\sigma_y}{\sigma_{av}})D \\ &= \tfrac{5}{16}(1 - \frac{1}{\gamma^2}\frac{\sigma_{cr,B}}{\sigma_y}\frac{\sigma_y}{\sigma_{av}})\gamma B \end{aligned} \tag{II.12}$$

where $\sigma_{cr,B}$ and $\sigma_{cr,D}$ are the elastic buckling stresses of legs *B* and *D* respectively.

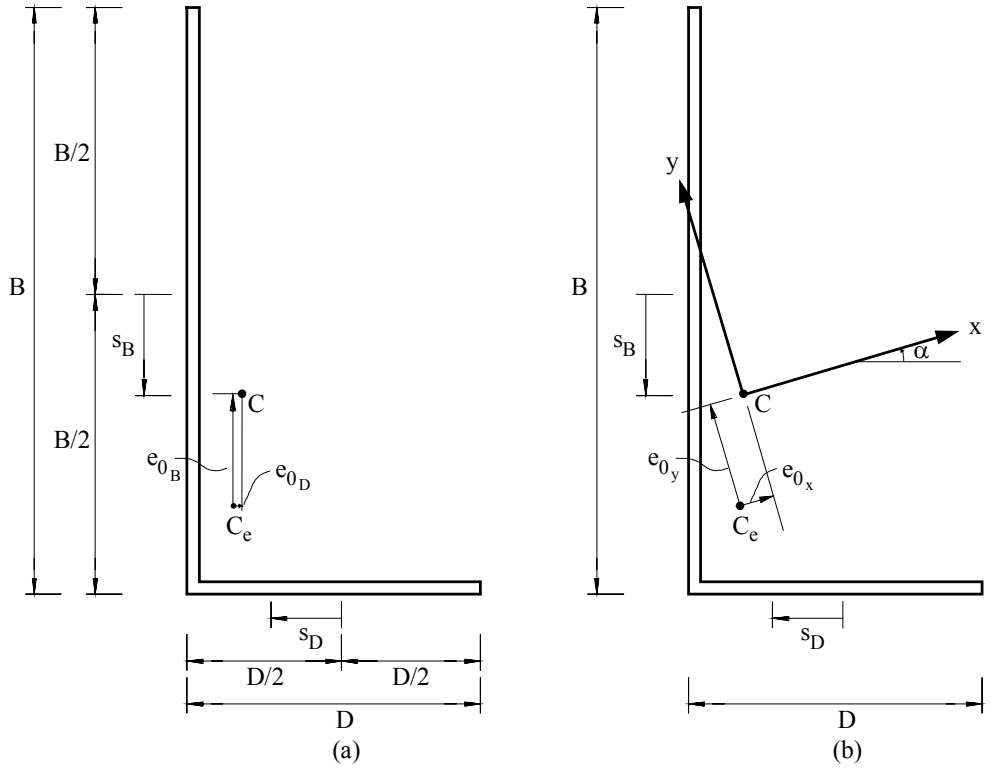

Figure II.3: Shift in the line of action of the force in an unequal angle

Obtaining the ultimate average stress according to Assumption (2) above, the shifts can be obtained as,

$$s_B = \begin{cases} 0 & \text{for } \lambda_{y,B} \le 1.22 \\ \tfrac{5}{16}\dfrac{\lambda_{y,B} - 1.22}{\lambda_{y,B} - 0.22}B & \text{for } \lambda_{y,B} > 1.22 \end{cases} \tag{II.13}$$

$$s_D = \begin{cases} 0 & \text{for } \lambda_{y,B} \le 0.22 + 1/\gamma^2 \\ \frac{5}{16}\dfrac{\lambda_{y,B} - (0.22 + 1/\gamma^2)}{\lambda_{y,B} - 0.22}\gamma B & \text{for } \lambda_{y,B} > 0.22 + 1/\gamma^2 \end{cases} \quad \text{(II.14)}$$

where $\lambda_{y,B}$ and is the plate slenderness of leg B.

Having obtained the location of the resultant force of each leg, the shifts of the resultant force (P) of the cross-section in directions parallel to the legs (see Fig. II.3a) are given by,

$$e_{0B} = \frac{s_B}{1+\gamma} \quad \text{(II.15)}$$

$$e_{0D} = \frac{\gamma s_D}{1+\gamma} \quad \text{(II.16)}$$

The eccentricities of the force (P) relative to the gross-section centroid (C) in the principal directions are then,

$$e_{0x} = \frac{1}{1+\gamma}\left[s_B \sin\alpha + \gamma s_D \cos\alpha\right] \quad \text{(II.17)}$$

$$e_{0y} = \frac{1}{1+\gamma}\left[s_B \cos\alpha - \gamma s_D \sin\alpha\right] \quad \text{(II.18)}$$

where α is the counter-clockwise angle between leg D and the principal x-axis, as shown in Fig. II.3b. For an unequal angle, the angle (α) is given by,

$$\alpha = \tfrac{1}{2}\tan^{-1}\left(\frac{6\gamma^2}{-\gamma^4 - 4\gamma^3 + 4\gamma + 1}\right), \quad \gamma \le 1 \quad \text{(II.19)}$$

As shown in Fig. II.4, for $0.5 \le \gamma \le 1$, eqn. (A19) can be approximated closely by

$$\alpha \approx 1.05\gamma - 0.2625, \quad 0.5 \le \gamma \le 1, \quad \text{(II.20)}$$

where α is in radian.

The eccentricities e_{0x} and e_{0y} given by eqns (II.17) and (II.18) respectively induce bending about the principal y-axis and x-axis respectively in a pin-ended unequal angle column.

For unequal angles with rounded corners ($r_i \neq 0$), the expressions for e_{0x} and e_{0y} are associated with a small error.

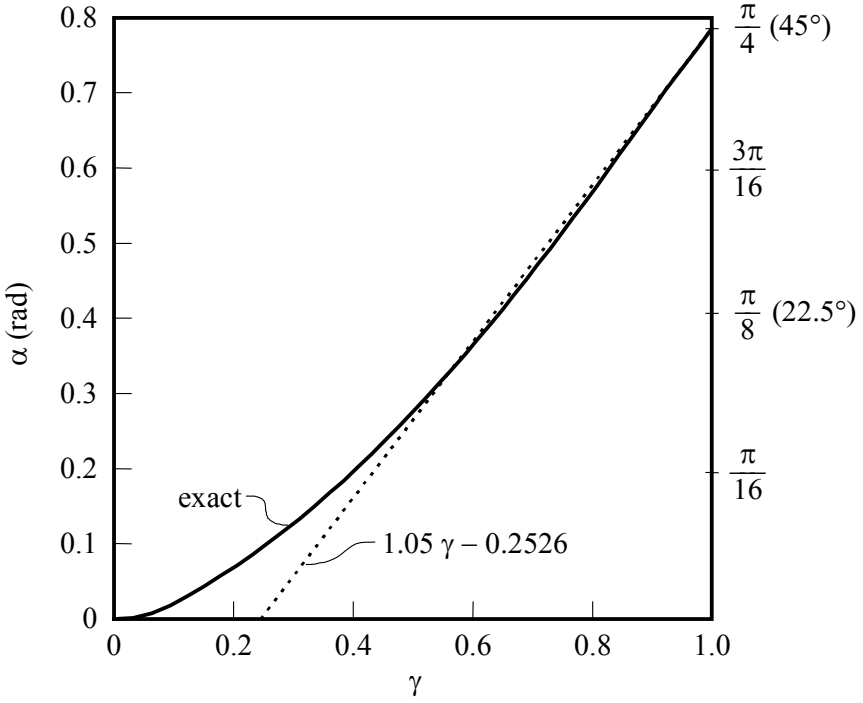

Figure II.4: Exact and approximate functions for the rotation (α) vs leg length ratio (γ)

Appendix III. Sample calculations of P_9 and $P_{n,r}$ design strengths

Example: Wilhoite angle section, column length of 1227mm

$m := 1L$ $sec := 1T$ $kg := 1M$ $N := 1L \cdot \frac{1M}{1T^2}$ $mm := \frac{m}{10^3}$ $MPa := \frac{N}{mm^2}$ $kN := 10^3 \cdot N$

This Mathcad worksheet determines the capacity of a pin-ended angle column of length 1227 mm loaded through the gross section centroid. According to the AISI Specification, such a column shall be treated as eccentrically loaded with an eccentricity based on the shift in the effective centroid. The following example uses an accurate expression for the shift in the effective centroid, and also uses accurate effective width equations for determining the bending capacity. In addition, the worksheet calculates the strength by reducing the column axial capacity by a factor β.

Worksheet prepared by Kim Rasmussen.

A Geometric and material properties

$B := 69.3 \cdot mm$ $t := 3.00 \cdot mm$ $r_i := 3 \cdot mm$

$L := 1227 \cdot mm$ $K_{y2} := 1$ $K_{x2} := 1$

$F_y := 465 \cdot MPa$ $E := 203000 \cdot MPa$ $\nu := 0.3$

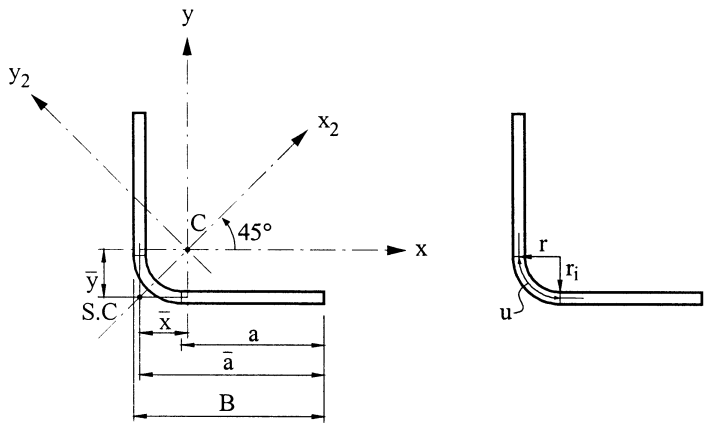

B Gross section constants (refer to AISI Design Manual for formulae)

1 Basic parameters

$r := r_i + \frac{t}{2}$ $\quad r = 4.5\,mm$

$a := B - \left(r + \frac{t}{2}\right)$ $\quad a = 63.3\,mm$

$a\_bar := B - \frac{t}{2}$ $\quad a\_bar = 67.8\,mm$

$u := \frac{\pi \cdot r}{2}$ $\quad u = 7.069\,mm$

2 Cross-sectional area

$A := t \cdot (2 \cdot a + u)$ $\quad A = 401.006\,mm^2$

3 Distance between centroid and centrelines of webs

$x\_bar := \frac{t}{A} \cdot \left[a \cdot \left(\frac{a}{2} + r\right) + u \cdot (0.363 \cdot r)\right]$ $\quad x\_bar = 17.206\,mm$

$y\_bar := x\_bar$ $\quad y\_bar = 17.206\,mm$

4 Moment of inertia about x and y axes

$I_x := t \cdot \left[a \cdot \left(\frac{a}{2} + r\right)^2 + \frac{a^3}{12} + u \cdot (0.363 \cdot r)^2 + 0.149 \cdot r^3\right] - A \cdot x\_bar^2$ $\quad I_x = 1.93 \times 10^5\,mm^4$

$I_y := I_x$ $\quad I_y = 1.93 \times 10^5\,mm^4$

5 Product of inertia about x and y axes

$I_{xy} := t \cdot \left[-0.137 \cdot r^3 + u \cdot (0.363 \cdot r)^2\right] - A \cdot x\_bar \cdot y\_bar$ $\quad I_{xy} = -1.187 \times 10^5\,mm^4$

6 Moment of inertia about x2 and y2 axes

$I_{y2} := I_x + I_{xy}$ $\quad I_{y2} = 7.427 \times 10^4\,mm^4$

$I_{x2} := I_x - I_{xy}$ $\quad I_{x2} = 3.117 \times 10^5\,mm^4$

7 Radii of gyration about x2 and y2 axes and polar radius of gyration

$$r_{y2} := \sqrt{\frac{I_{y2}}{A}} \qquad r_{y2} = 13.609\,\text{mm}$$

$$r_{x2} := \sqrt{\frac{I_{x2}}{A}} \qquad r_{x2} = 27.878\,\text{mm}$$

$$r_0 := \sqrt{\frac{(I_{y2} + I_{x2})}{A}} \qquad r_0 = 31.022\,\text{mm}$$

8 St Venant torsion constant

$$J := \frac{t^3}{3}\cdot(2\cdot a + u) \qquad J = 1.203 \times 10^3\,\text{mm}^4$$

9 Distance from centroid to shear centre

$$x_0 := -(x\_bar\cdot\sqrt{2}) \qquad x_0 = -24.332\,\text{mm}$$

10 Monosymmetry parameter

$$r_1 := \sqrt{r_0^{\,2} + x_0^{\,2}} \qquad r_1 = 39.427\,\text{mm}$$

$$\beta := 1 - \left(\frac{x_0}{r_1}\right)^2 \qquad \beta = 0.619$$

11 Section modulus

$$c_{tip} := \frac{B}{\sqrt{2}} - \left(\sqrt{2}\cdot x\_bar + \frac{t}{2\cdot\sqrt{2}}\right) \qquad c_{tip} = 23.61\,\text{mm}$$

$$c_{heel} := r_i + t + \left(x\_bar - r_i - \frac{t}{2}\right)\cdot\sqrt{2} \qquad c_{heel} = 23.968\,\text{mm}$$

$$S_y := \frac{I_{y2}}{\max(c_{tip}, c_{heel})} \qquad S_y = 3.099 \times 10^3\,\text{mm}^3$$

C Calculation of axial capacity using beam-column approach (design model P9)

1 Overall flexural buckling stress (ignoring torsion)

$$F_{ey2} := \frac{\pi^2 \cdot E}{\left(\frac{K_{y2} \cdot L}{r_{y2}}\right)^2} \qquad F_{ey2} = 246.476\,\text{MPa}$$

$$\lambda_c := \sqrt{\frac{F_y}{F_{ey2}}} \qquad \lambda_c = 1.374$$

$$F_{ny2} := \text{if}\left[\lambda_c \le 1.5, \left(\left(0.658^{\lambda_c^2}\right)\right) \cdot F_y, \left[\left(\frac{0.877}{\lambda_c^2}\right) \cdot F_y\right]\right] \qquad F_{ny2} = 211.115\,\text{MPa}$$

2 Effective area in compression at Fny2

$$k_c := 0.43$$

$$F_{cr\_c} := \frac{k_c (\pi)^2 \cdot E}{12 \cdot \left(1 - \nu^2\right)} \cdot \left(\frac{t}{a}\right)^2 \qquad F_{cr\_c} = 177.205\,\text{MPa}$$

$$\lambda := \sqrt{\frac{F_{ny2}}{F_{cr\_c}}} \qquad \lambda = 1.091$$

$$\rho := \frac{\left(1 - \frac{0.22}{\lambda}\right)}{\lambda} \qquad \rho = 0.732$$

$$A_e := t \cdot (2 \cdot \rho \cdot a + u) \qquad A_e = 299.034\,\text{mm}^2$$

3 Concentric column capacity

$$P_{nc} := A_e \cdot F_{ny2} \qquad P_{nc} = 63.131\,\text{kN}$$

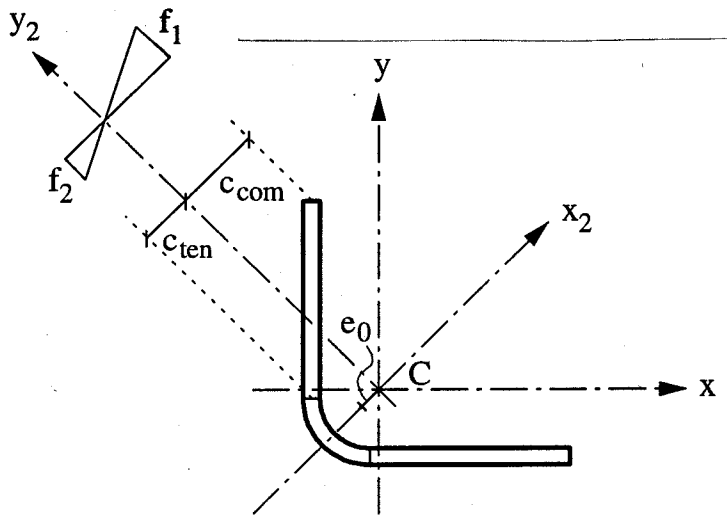

4 Section modulus of effective area in bending for compression at the flange tips (using the Bambach-Rasmussen effective width equations)

$c_{com} := \frac{B}{\sqrt{2}} - \sqrt{2}\cdot\left(x\_bar + \frac{t}{2}\right)$ $c_{com} = 22.549\,mm$

$c_{ten} := \frac{a}{\sqrt{2}} - c_{com}$ $c_{ten} = 22.211\,mm$

$f_1 := F_y$ (compression stress) $f_1 = 465\,MPa$

$f_2 := \frac{c_{ten}}{c_{com}}\cdot F_y$ (tension stress) $f_2 = 458.033\,MPa$

$\psi := \frac{f_2}{f_1}$ $\psi = 0.985$

$k_b := 0.57 + 0.21\cdot\psi + 0.07\cdot\psi^2$ $k_b = 0.845$

$F_{cr\_b} := \frac{k_b(\pi)^2\cdot E}{12\cdot\left(1-\nu^2\right)}\cdot\left(\frac{t}{a}\right)^2$ $F_{cr\_b} = 348.135\,MPa$

$\lambda := \sqrt{\frac{F_y}{F_{cr\_b}}}$ $\lambda = 1.156$

$\rho := if\left[\frac{(1+\psi)}{\lambda}\cdot\left[1-0.22\cdot\left[\frac{(1+\psi)}{\lambda}\right]\right] > 1,1,\frac{(1+\psi)}{\lambda}\cdot\left[1-0.22\cdot\left[\frac{(1+\psi)}{\lambda}\right]\right]\right]$ $\rho = 1$

The section is fully effective in bending

$S_{ey} := S_y$ $S_{ey} = 3.099\times10^3\,mm^3$

5 Minor axis bending capacity

$M_n := S_{ey} \cdot F_y$ $\quad M_n = 1.441 \times 10^3\,\text{kN}\cdot\text{mm}$

6 Determine the shift of the line of action of the internal force (based on Stowell's expression for the stress distribution in an outstand)

$\lambda_{cy} := \sqrt{\frac{F_y}{F_{cr\_c}}}$ $\quad \lambda_{cy} = 1.62$

$e_0 := \frac{5}{16\cdot\sqrt{2}} \cdot \frac{(\lambda_{cy} - 1.22)}{(\lambda_{cy} - 0.22)} \cdot a$ $\quad e_0 = 3.996\,\text{mm}$

7 Determine axial capacity by solving the quadratic interaction equation

$P_E := F_{ey2} \cdot A$ $\quad P_E = 98.838\,\text{kN}$

$AA := \frac{1}{P_{nc} \cdot P_E}$ $\quad AA = 1.603 \times 10^{-4}\,\frac{1}{(\text{kN})^2}$

$BB := -\left(\frac{1}{P_{nc}} + \frac{e_0}{M_n} + \frac{1}{P_E}\right)$ $\quad BB = -0.029\,\frac{1}{\text{kN}}$

$CC := 1$

$P_n := \frac{\left[-BB - \sqrt{(BB^2 - 4\cdot AA\cdot CC)}\right]}{2\cdot AA}$ $\quad P_n = 47.27\,\text{kN}$

Thus, the capacity of the columns is: $P_n = 47.27\,\text{kN}$

This value can be compared with the test values obtained for the same cross-section by Wilhoite et al (1984) of 58.3kN, 60.1 kN and 65.0 kN.

D Calculation of axial capacity ($P_{n,r}$) using direct approach

1 Overall flexural buckling stress (ignoring torsion)

$$F_{ey2} := \frac{\pi^2 \cdot E}{\left(\frac{K_{y2} \cdot L}{r_{y2}}\right)^2} \qquad F_{ey2} = 246.476\,\text{MPa}$$

$$\lambda_c := \sqrt{\frac{F_y}{F_{ey2}}} \qquad \lambda_c = 1.374$$

$$F_{ny2} := \text{if}\left[\lambda_c \le 1.5, \left(\left(0.658^{\lambda_c^2}\right)\right) \cdot F_y, \left[\left(\frac{0.877}{\lambda_c^2}\right) \cdot F_y\right]\right] \qquad F_{ny2} = 211.115\,\text{MPa}$$

2 Effective area in compression at Fny2

$$k_c := 0.43$$

$$F_{cr\_c} := \frac{k_c (\pi)^2 \cdot E}{12 \cdot \left(1 - \nu^2\right)} \cdot \left(\frac{t}{a}\right)^2 \qquad F_{cr\_c} = 177.205\,\text{MPa}$$

$$\lambda := \sqrt{\frac{F_{ny2}}{F_{cr\_c}}} \qquad \lambda = 1.091$$

$$\rho := \frac{\left(1 - \frac{0.22}{\lambda}\right)}{\lambda} \qquad \rho = 0.732$$

$$A_e := t \cdot (2 \cdot \rho \cdot a + u) \qquad A_e = 299.034\,\text{mm}^2$$

3 Concentric column capacity

$$P_{nc} := A_e \cdot F_{ny2} \qquad P_{nc} = 63.131\,\text{kN}$$

4 Reduction factor (β)

$$\lambda_{cy} := \sqrt{\frac{F_y}{F_{cr\_c}}} \qquad \lambda_{cy} = 1.62$$

$$\beta := \text{if}\left[\lambda_{cy} \le 1.22, 1, \frac{0.68}{\left(\lambda_{cy} - 1\right)^{0.25}}\right] \qquad \beta = 0.766$$

5 Column strength accounting for the effect of the shift in the effective centroid

$$P_{n\_r} := \beta \cdot P_{nc} \qquad P_{n\_r} = 48.38\,\text{kN}$$

Thus, the capacity of the columns is: $P_{n\_r} = 48.38\,\text{kN}$

This value can be compared with the value of 47.27 kN obtained using a beam-column approach, and the test values obtained for the same cross-section by Wilhoite et al (1984) of 58.3kN, 60.1 kN and 65.0 kN.